62235 POIKILITIC IMPACT MELT 320 g

INTRODUCTION: 62235 is a homogeneous, coherent block (Fig. 1) composed of poikilitic, KREEP-rich melt with a few clasts and small vesicles. It was collected from the rim of Buster Crater where it was perched and its orientation documented. Zap pits are irregularly distributed with many on one side and few on the others.

FIGURE 1. S-72-38383.

PETROLOGY: Crawford and Hollister (1974) give a detailed petrographic description with mineral analyses. Vaniman and Papike (1981) include 62235 in a study of highland melt rocks. The rock is composed of ~57% calcic plagioclase with the remainder mainly

elongate oikocrysts of hypersthene (Fig. 2). The oikocrysts are up to ~1 mm long and are often cored with unzoned olivine and overgrown with pigeonite. Some lamellae and patches of augite are also present within the oikocrysts. Mineral compositions are shown in Figure 3; the early hypersthene is aluminous (~3% Al_2O_3). Interoikocryst areas are composed mainly of plagioclase, glass, ilmenite (or armalcolite?) and Fe-metal/troilite (Fig. 2). Pearce et al. (1976) show that Fe-metal composes 1.1% of the rock and has compositions within the meteoritic range (Fig. 4). A crystallization sequence of plagioclase → pyroxene → ilmenite was deduced by Engelhardt (1978, 1979).

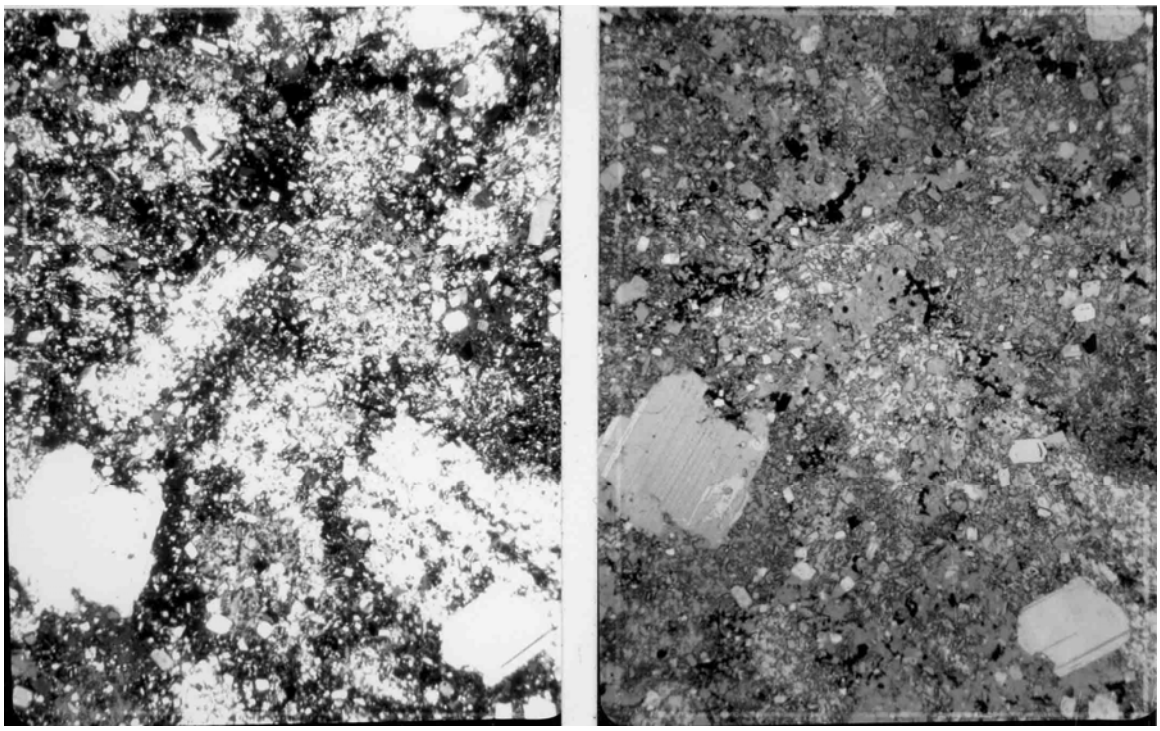

FIGURE 2. 62235,65, general view. Width 2 mm.
a) xpl. b) ppl with reflector in.

Plagioclase occurs in several forms: (i) as large, shocked or polygonal clasts (An_{94-96}), (ii) as small, euhedral, blocky grains (An_{98}) with visible, more sodic (<An_{90}) rims, (iii) as a second group of blocky grains (An_{84}), (iv) as small, rectangular chadacrysts and laths in the interoikocryst areas (An_{92-93}). All of the coarser blocky grains show reverse zoning in their outer rims to An_{92-93}, the same composition as the chadacrysts and interoikocryst laths. Crawford and Hollister (1974) give Fe/Mg data for plagioclase.

Simonds et al. (1976) find that 62235 contains 9% total clasts larger than 50 μm, and that 95% of these clasts are plagioclase. Meyer et al. (1974) analyzed minor elements in plagioclase using the ion microprobe (Table 1) and found that the Ba contents of plagioclases larger than 50 μm are much too low for the plagioclases to be in equilibrium with the melt. These low-Ba plagioclases are ~10% of 62235.

The characteristics of the rock require that most of it crystallized from a silicate melt, the rest being fragmental. Crawford and Hollister (1974) interpret all but the coarsest shocked plagioclases as having crystallized from the melt and cite several features as suggesting crystallization at depth. They infer a volcanic origin with a source at ~200 km. These interpretations are not unique and the evidence of Meyer et al. (1974) suggests that more of the plagioclase is fragmental and that some of the featured cited by Crawford and Hollister (1974) are due to clast-matrix interactions. The rock is very similar to the other poikilitic samples interpreted as impact melts.

CHEMISTRY: Major and trace element analyses are presented, with little specific comment, by Brunfelt et al. (1973), Hubbard et al. (1973), LSPET (1973), Laul et al. (1974) and Wanke et al. (1976). Moore et al. (1973) provide C data and Clark and radionuclide data. Chemically 62235 is a KREEP-rich, siderophile-rich rock (Table 1, Fig. 5) similar to several other poikilitic rocks. Crawford and Hollister (1974) suggest that the siderophiles are indigenous, but high contents are usually interpreted as meteoritic contamination (Laul et al. 1974). The carbon content of 2 ppm (Moore et al. 1973) is extremely low.

TABLE 1. Minor elements in 62235 plagioclase
(Meyer et al., 1974) (ppm except Na_2O, wt %).

	Na_2O	Li	Mg	K	Ti	Sr	Ba
6 xenocrysts	0.42	5	600	240	97	162	9
1 small grain	0.76	10	360	500	130	270	30

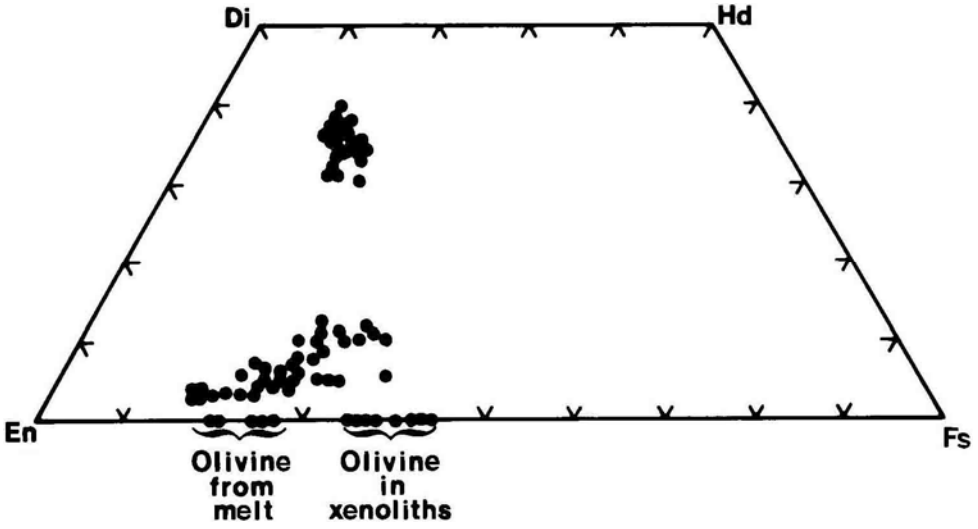

FIGURE 3a. Mineral compositions; from Crawford and Hollister (1974).

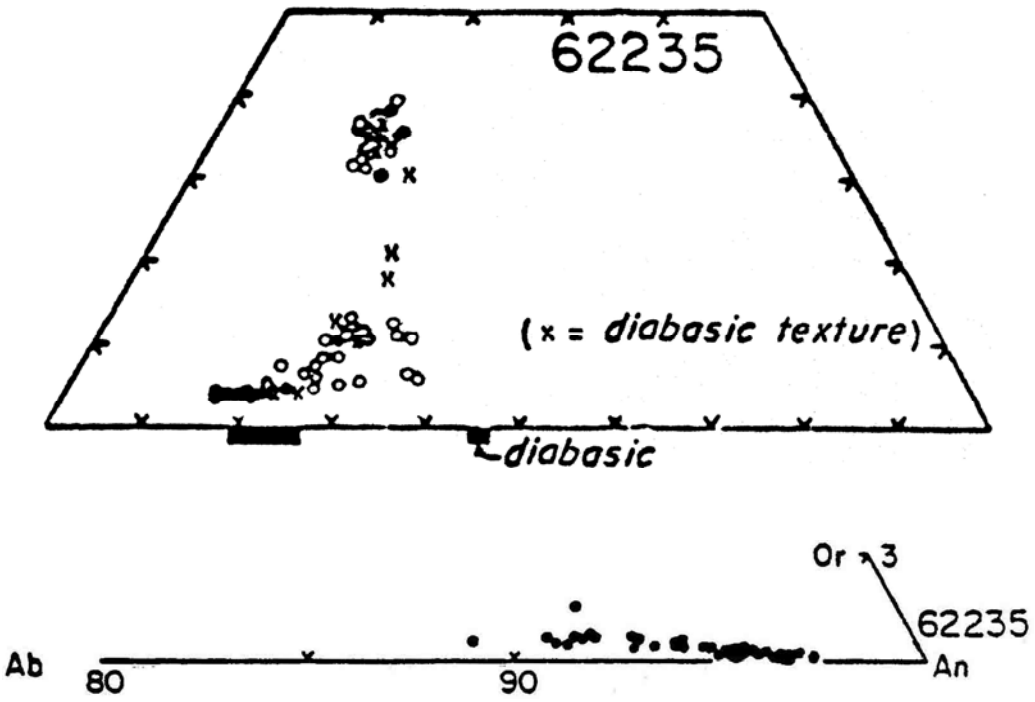

FIGURE 3b. Mineral compositions; from Vaniman and Papike (1981).

RADIOGENIC ISOTOPES AND GEOCHRONOLOGY: No internal isochron or ^{40}Ar-^{39}Ar data have been published. Nyquist et al. (1973) and Tera et al. (1974) provide whole-rock Rb-Sr isotopic data giving T_{BABI} ages of ~4.5 b.y. (Table 3).

Tera et al. (1974) provide U, Th, Pb isotopic data demonstrating the presence of much in situ radiogenic lead, as with many other KREEP samples. The sample falls on the U-Pb discord formed by most highland total rock samples, corresponding to a metamorphism age of ~3.9 b.y.

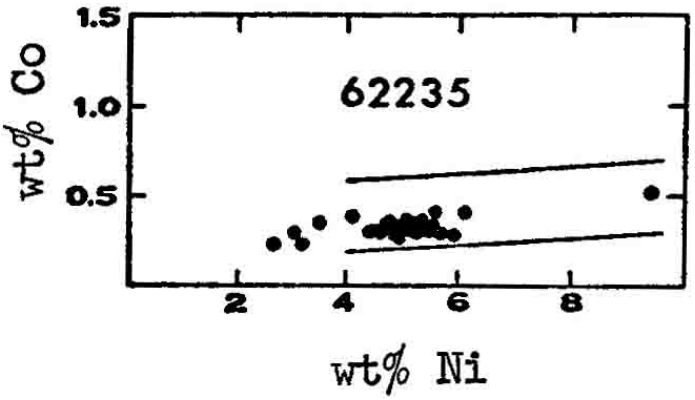

FIGURE 4. Metals; from Pearce et a1. (1976).

RARE GASES/EXPOSURE AGES: Drozd et al. (1974) provide ^{81}Kr-Kr, ^{21}Ne, and ^{38}Ar exposure ages of 153.9 ± 2.9, 104 ± 54 and 163.0 ± 54 m.y., respectively. However, the sample did not spend its entire 153 m.y. apparent exposure age at its surface location and it must have been lightly shielded. Pepin et al. (1974) show that the ^{21}Ne and ^{38}Ar ages (which depend on spallation production rates) agree with the ^{81}Kr-Kr age if the effective irradiation depth was 90 g/cm^2. Crozaz et al. (1974) use cosmic tracks to give a maximum exposure age (single point method) of 4 m.y. and a "true" suntan age (track density/depth method) of 2 m.y. There are large grain-to-grain track density variations. Morrison et al. (1973) use microcrater densities to suggest an exposure age of 2-3 m.y.

Lightner and Marti (1974b) provide xenon concentration and isotopic data without a specific interpretation.

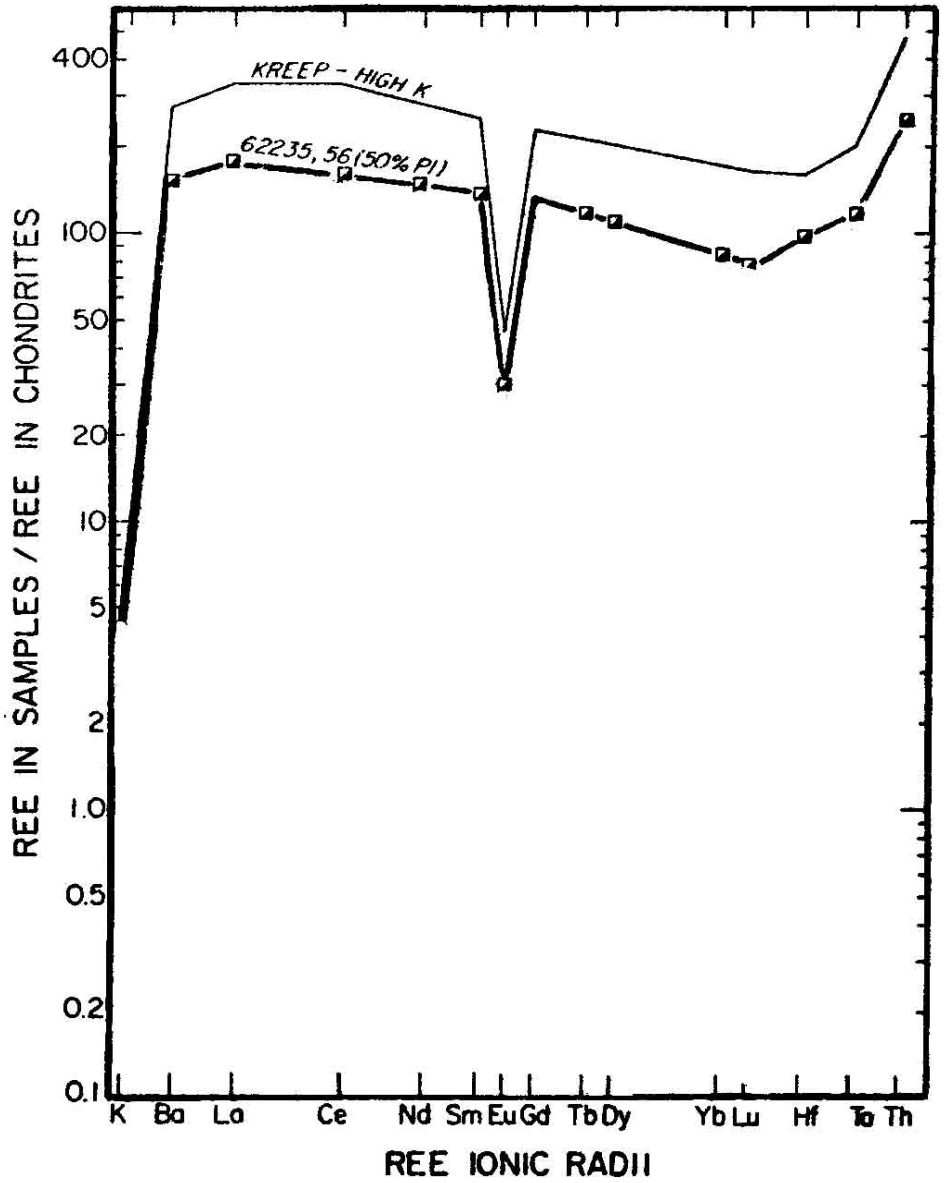

FIGURE 5. Incompatible elements; from Laul et al. (1974).

TABLE 2. Summary chemistry of 62235.

SiO_2	47.0
TiO_2	1.2
Al_2O_3	18.6
Cr_2O_3	0.19
FeO	9.5
MnO	0.11
MgO	10.3
CaO	11.5
Na_2O	0.48
K_2O	0.34
P_2O_5	0.40
Sr	160
La	60
Lu	2.7
Rb	9
Sc	16
Ni	700
Co	50
Ir ppb	19
Au ppb	17
C	2
N	
S	1000
Zn	2.2-11
Cu	3.9-11

Oxides in wt%; others in ppm except as noted.

TABLE 3. Rb-Sr data for 62235.

Rb ppm	Sr ppm	$^{87}Sr/^{86}Sr$	$^{87}Sr/^{86}Sr$*	T_{BABI}(b.y.)	Reference
9.32	161	0.70989±7	0.70042	4.48	Nyquist et al.(1973)
9.03	162	0.70944±9	0.70042	4.50	Tera et al.(1974)

*Calculated for 3.9 b.y., corrected for interlaboratory bias to Caltech data.

MICROCRATERS: Morrison et al. (1973) and Neukum et al. (1973) provide frequency distribution diagrams for microcraters (Fig. 6). Only about half the surface has microcraters and the rock was not continually tumbled. Morrison et al. (1973) conclude that the surface is well below steady-state for craters <0.08 cm in diameter. Neukum et al. (1973) conclude that 62235 has an equilibrium population. McDonnell et al. (1976) and Flavill et al. (1978) experimentally produced microcraters on a sample of 62235 by bombarding it with iron particles. They emphasize the importance of secondary ejecta.

PHYSICAL PROPERTIES: Collinson et al. (1973) provide NRM data for 62235 (Fig. 7) which they discuss further in Stephenson et al. (1974,1975) and Stephenson and Collinson (1974). They find two components of stable magnetization, one of which is extremely hard and of unusually high intensity. Investigation of paleointensity using the Thellier method suggests a field of 1.2 Oe, and using the anhysteretic remanent magnetization (ARM) method suggests a field of 1.4 Oe. Cisowski et al. (1975) used the data to give a field of 0.3 Oe using the IRMs method, later revised to 1.0 Oe (Cisowski et al., 1977). These results have been questioned: Brecher (1975) attributes the data to "textural remanance," not to any lunar field, and Pearce et al. (1976) performed heating experiments showing that complexities introduced by Fe-metal and troilite grains make the definition of paleointensity extremely difficult. Contrarily, Hargraves and Dorety (1976) interpret the small variation of NRM and IRM with alternating field demagnetization of 62235 to show that it is a good sample for paleointensity determinations.

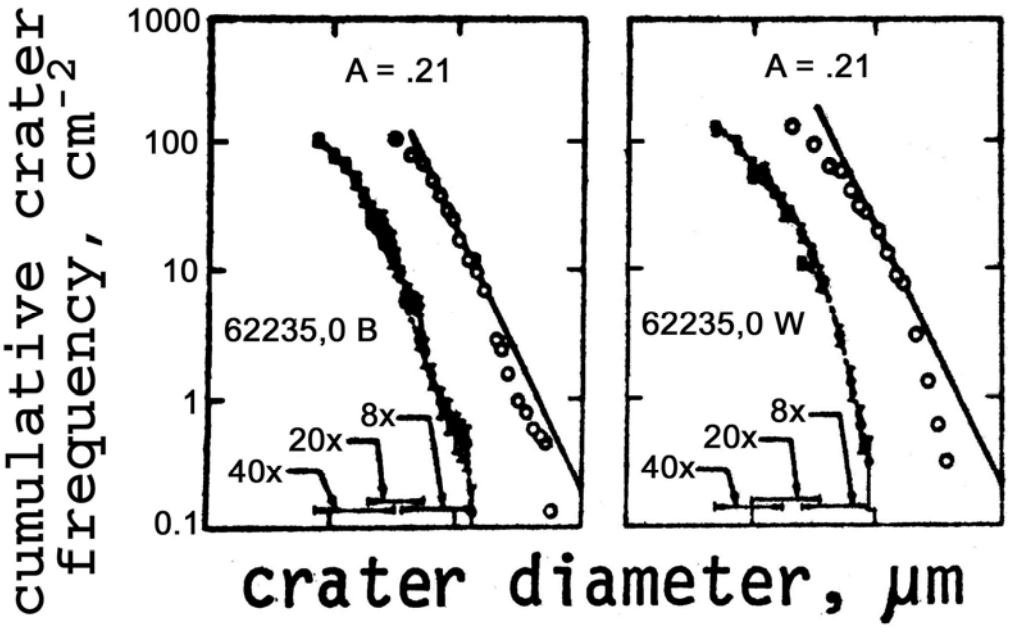

FIGURE 6. Microcraters; from Neukum et al. (1973).

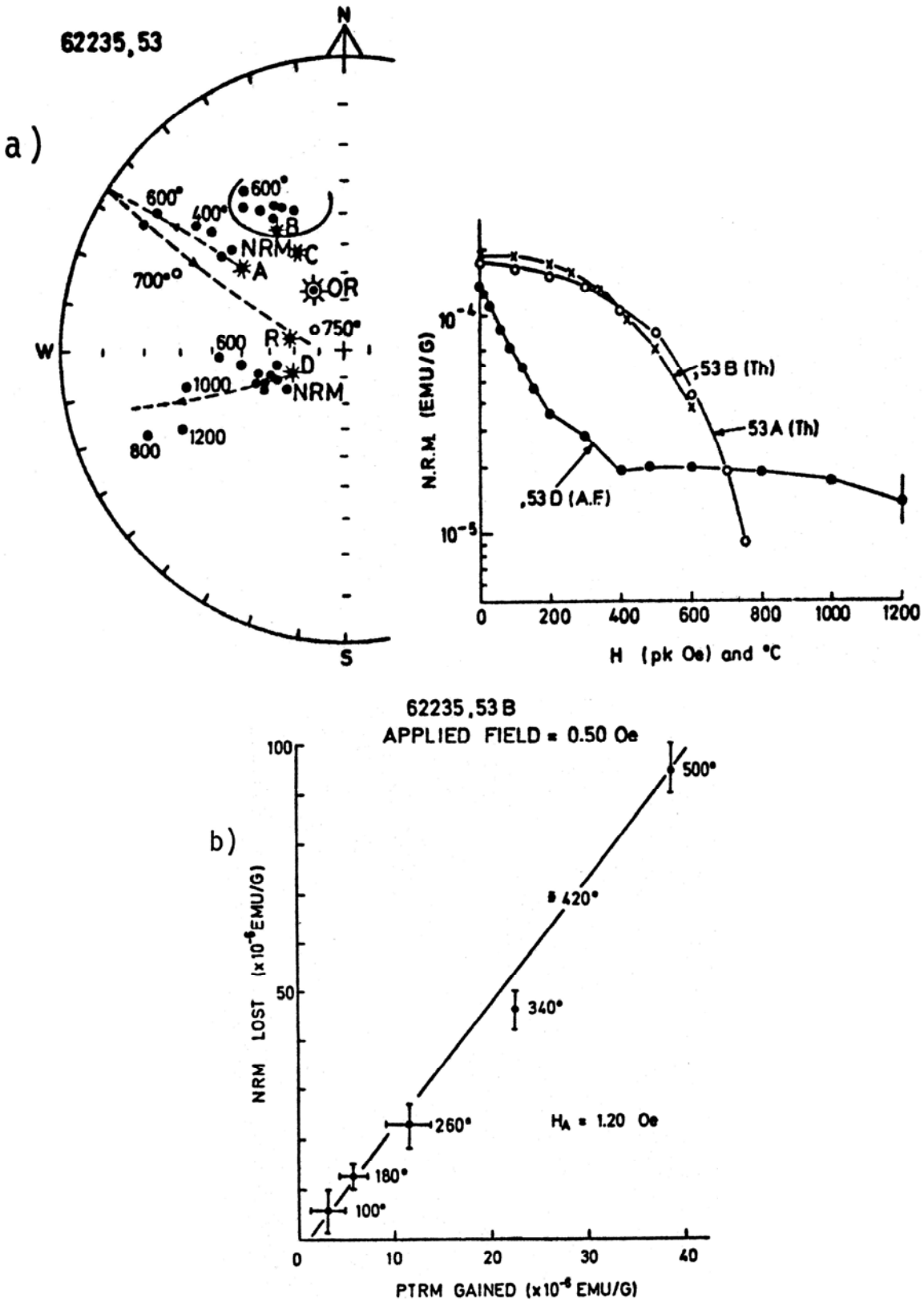

FIGURE 7. Magnetic data; from Collinson et al. (1973).
a) Alternating field and thermal magnetization. b) Field intensity determination.

Chung and Westphal (1973) provide dielectric constants, dielectric losses, and electrical conductivities for 62235 as functions of frequency and temperature (Fig. 8)

PROCESSING AND SUBDIVISIONS: In 1972, 62235 was sawn to produce a slab and two end-pieces (Fig. 9). End piece ,12 and the slab ,13 were split and substantially allocated (Figs. 9, 10). A few splits are from the ,11 end piece.

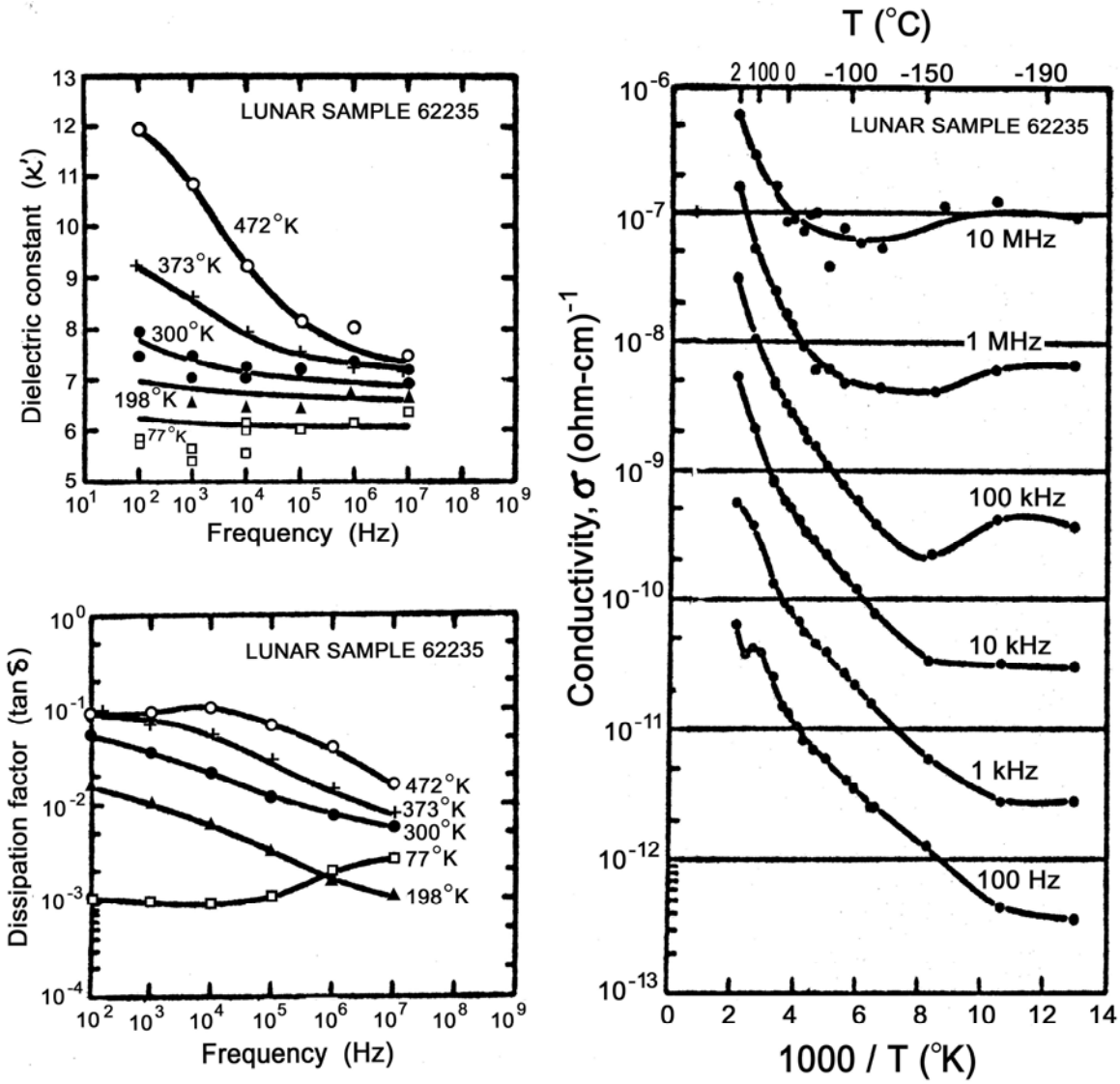

FIGURE 8. Electrical data; from Chung and Westphal (1973).

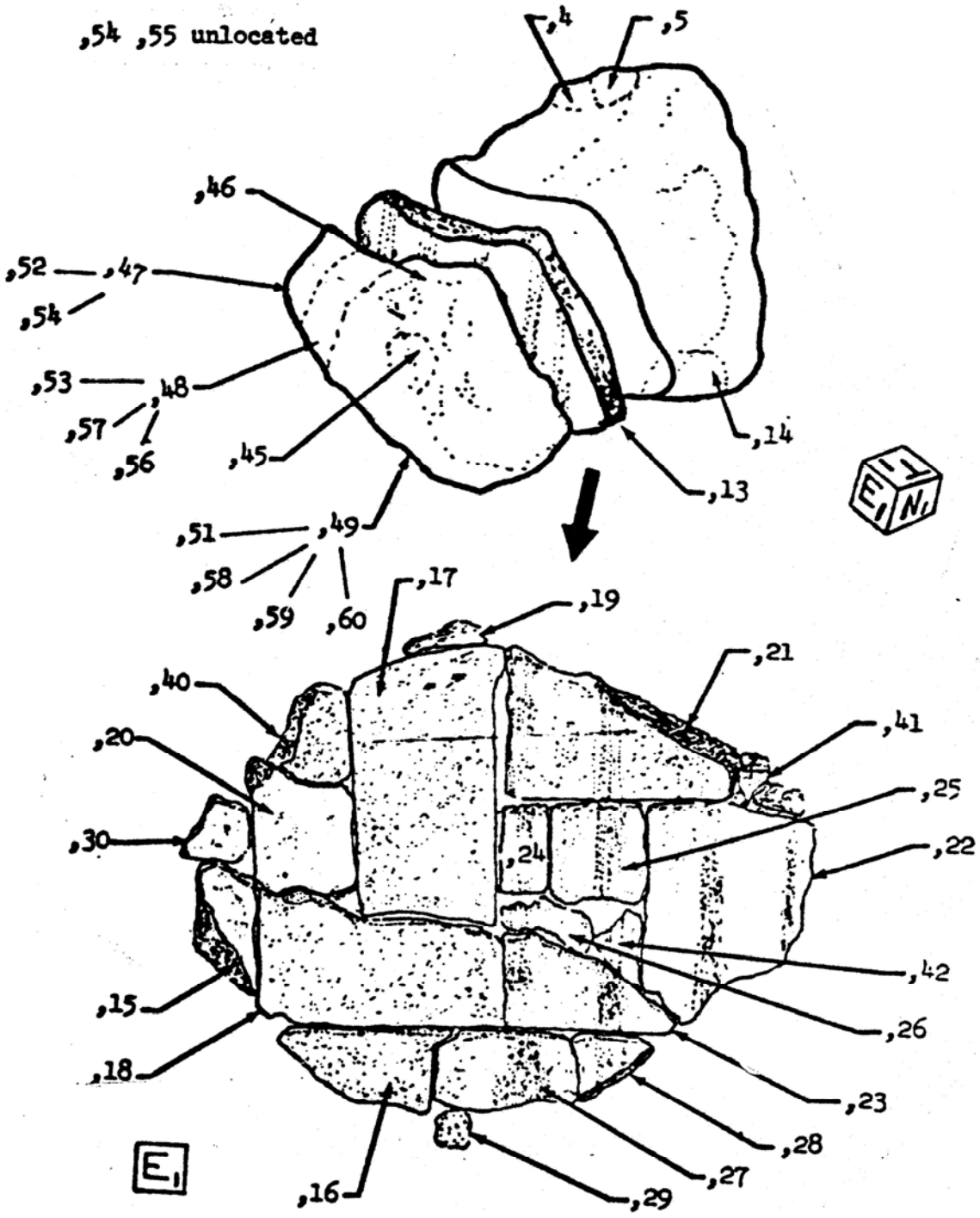

FIGURE 9. Cutting diagram.

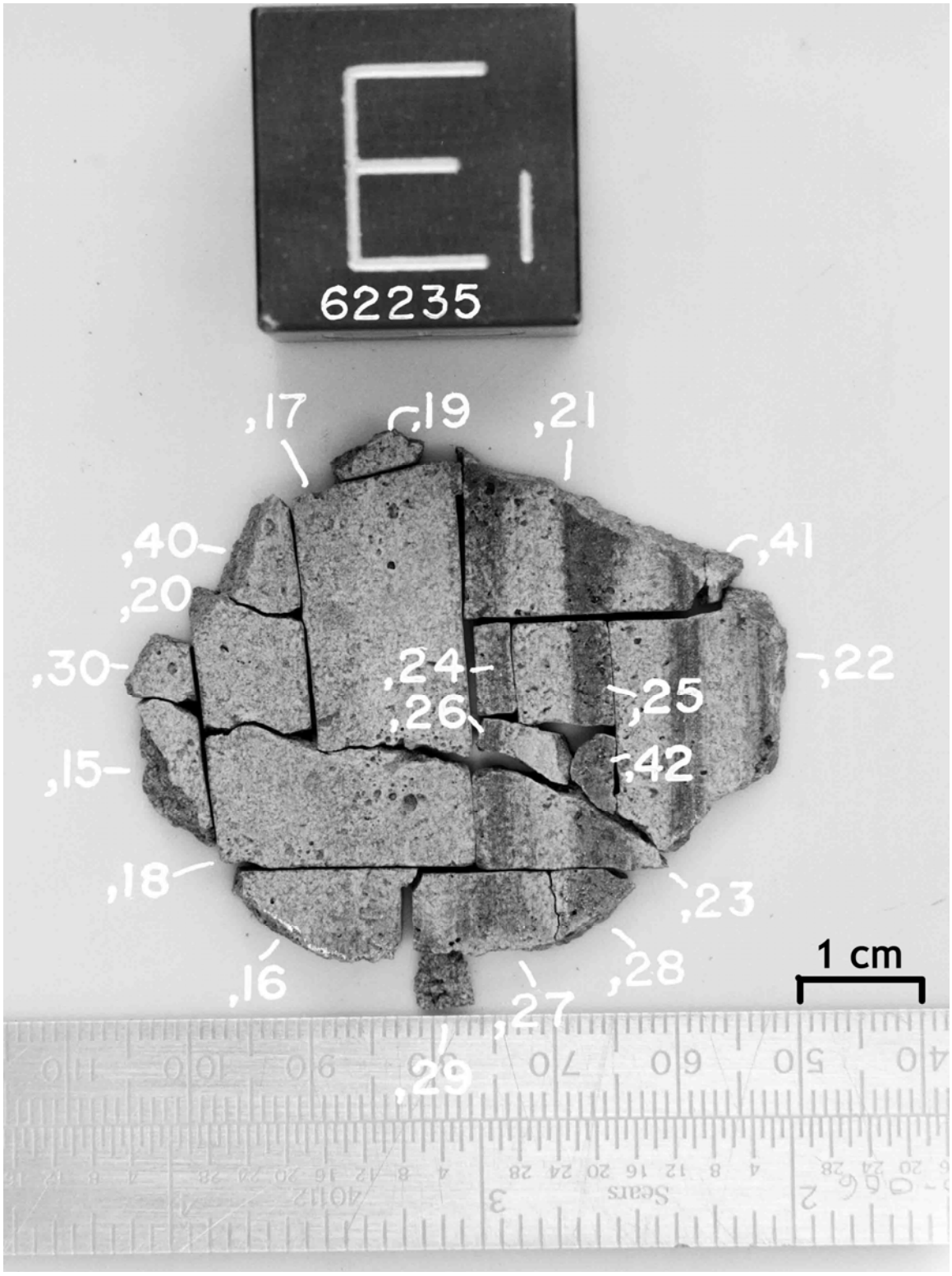

FIGURE 10. Slab subdivision. S-72-53515.